Effect analysis on energy conversion enhancement and NOx emission reduction of ammonia/hydrogen fuelled wavy micro-combustor for micro-thermophotovoltaic application

Lei Han[a, b], Junwei Li[a,*], Dan Zhao[b], Yunzhi Xi[a], Xingpeng Gu[a], Ningfei Wang[a]

[a] *School of Aerospace Engineering, Beijing Institute of Technology, Beijing 100081, China*

[b] *Department of Mechanical Engineering, College of Engineering, University of Canterbury, Christchurch 8140, New Zealand*

Author Email:

docarezone@hotmail.com (Lei Han)

dan.zhao@canterbury.ac.nz (Dan Zhao)

xyzhiii@163.com (Yunzhi Xi)

1975564047@qq.com(Xingpeng Gu)

wangningfei@bit.edu.cn (Ningfei Wang)

** Corresponding author Email:*

david78lee@gmail.com (Junwei Li).

Abstract

Ammonia (NH_3) is regarded as an alternative fuel not only as a carbon-free fuel but also as a renewable hydrogen-carrier. It is possible that the safety in micro-combustor can be improved through partial NH_3 substitution for hydrogen. However, knowledge of the thermal performance and nitrogen oxides (NOx) emission of ammonia/hydrogen combustion, especially in the micro-combustor, has been insufficient. In order to enhance thermal performance, reduce NOx emission and improve flame stabilization of ammonia/hydrogen fuelled micro-combustors for thermophotovoltaic (TPV) application, three types of micro-combustors with a wavy profile are designed and evaluated. For this, a three-dimensional (3D) numerical model with a detailed chemical reaction mechanism has been verified and applied to assess the thermal performance of the modified micro combustors in terms of the outer wall temperature distributions. The average temperature of these wavy combustors is found to be much higher than that of the conventional smooth combustor, regardless of the hydrogen/ammonia mixture flow velocity. Moreover, the wavy is a more effective measure to improve temperature uniformity when the mixture velocity is greater than 12m/s. Comparing the flame stability behaviours of hydrogen/ammonia/air blended combustion in both the conventional and the proposed wavy combustors reveals that the blowout limit is effectively broadened. Finally, the effects of 1) hydrogen/ammonia blended ratio and 2) fuel-air equivalence ratio on NO_x emissions are examined in detail. It is found that approximately 21.2% of NOx emission reduction could be achieved in the ARC wavy micro-combustor. NOx emission reduction can be gradually improved, as the nitrogen fuel mass ratio is increased. This present research sheds lights on an effective design of a micro-combustor with enhanced thermal performance and reduced NOx emission.

Key words: *energy conversion performance; blended fuel; micro-combustion; wavy profile; blowout limit; NOx emissions.*

1. Introduction

Ammonia (NH_3) is regarded as an alternative fuel not only as a carbon-free fuel but also as a renewable hydrogen-carrier. NH_3 is also considered as a clean and high density hydrogen carrier since it can be easily rendered liquid at atmospheric temperature and because of its lower cost of storage and production, distribution and transportation [1]. Besides, NH_3 is able to burn directly with blends fuel or additives [2]. It is possible that the safety of hydrogen (H_2) use in combustor can be improved through partial NH_3 substitution for hydrogen. With the increasing demand of worldwide industries for portable energy conversion and power-harnessing in smaller-scale applications, micro power generators (MPG) are developed using micro or nanotechnologies to convert different forms of energy into electricity energy [3]. In recent years, it is essential to establish efficient approaches for designing and manufacturing energy-efficient and environmentally-friendly solutions for MPG. The micro-thermophotovoltaic (MTPV) [4, 5] is one kind of micro-combustion-based MPG attracting extensive attention due to its reliability, longevity and simple structure without moving parts, and is suitable for use in commercial electronics and personal micro devices [6]. Researcher has experimentally evaluated the feasibility of using ammonia-hydrogen blend-fuelled as green fuel in MTPV

device with GaSb, modifying a previous hydrocarbon fuel combustor for MTPV [7].

Combustion of hydrogen or mixture fuels provides a much higher energy density due to the significant reduction in weight or volume of combustor chamber compared with portable lithium-ion batteries [8]. Temperature distribution characteristics are key points to improve the combustor efficiency [9] and the performance of the MTPV. The major challenges faced in optimizing the micro-combustor's ability to convert chemical fuels into electricity energy are not only to achieve uniform and high temperature distribution [10] and wider flammability limit [11] but also to obtain higher emission efficiency of exhaust gas [12].

One of the most important issues for optimization of combustor is to improve its outer wall thermal performance, which attracts considerable experimental and numerical investigations due to its direct effect on feasibility and demanded energy conversion efficiency. Various new methods have been applied to combustors by employing fins or bluff body [13, 14], catalytic combustion [15], porous media [16-18], counter-flow [19], and heat recirculation [20, 21]. Peng et al. [16] inserted a porous media into a combustor to augment the wall temperature and subsequently enhanced the applied radiation energy of MTPV. This is attributed to the solid matrix of porous media offering a better thermal characteristic (heat capacity, conductivity, and emissivity) than gas. Yan [22]

and Yilmaz [12] reported that adjusting the angle and width of the bluff body can improve the combustion efficiency and blowout effectively. Li and Hong [23] conducted numerical study of H_2/CH_4/air blended combustion and concluded that the output electrical energy of the combustor with the implementation of catalyst (Pt) is increased by up to 23.8% compared with that without the catalyst. They also revealed that the catalyst has adverse effects on combustion process at higher mass flow rates. The objective of Akhtar's [24] research was to investigate the impact of different cross-section types (including circular, rectangular, square, trapezoidal and triangular) on the outer wall temperature distribution and the flame structure of hydrogen fuelled micro-combustor. The results showed that trapezoidal and the triangular cross-sections brings about better thermal performance and overall energy conversion efficiency for the low flow rates and high flow rates respectively. Zuo et al. [25] studied the positive effects of H_2/air premixed flame in the combustor improved by gradually varying the diameter. Mansouri et al. [26] proposed configuration with wavy profiles as thermal performance enhancement for flat micro-combustor. The significant impact brought by the above-mentioned optimization of inner combustor on the thermal performance was observed. The lack of an easy implement approach to improve the thermal performance of micro combustors partially motivated the present work.

Blowout limits [8, 27] of micro-combustors need to be considered for feasible industry operation by researchers and engineers. The residence time of gas mixture decreases as combustor size decreases. Furthermore, excessive heat loss from the outer wall of combustor will suppress flame stability and even result in blow out [28]. Massive research has been conducted to extend the flame stability of the conventional micro-combustors [8, 27, 29]. Therefore, the current topic of interest lies in approaches that are able to effectively broaden blowout limit and enhance thermal performance.

In several previous studies [10, 30-35], ammonia/hydrogen was seen as one of the promise fuel and it was actually used for combustor design. NO_X emissions produced via combustion present significant risks to both health and the environment. Therefore, although ammonia is an important enhancer of combustion, there is a large NOx proportion of emissions using this fuel [36]. Cai et al. [37] conducted numerical investigation on the performances and NO emission characteristics of ammonia/oxygen premixed combustion. Xiao et al. [38] and Rocha and Ramos [39, 40] reported a study of detailed mechanisms of ammonia/air to represent the reaction kinetics and NO emission under combustor conditions. Li et al. [41] found that the NOx emission increases sharply with the NH_3 addition mainly through the enhanced HNO pathway in the main reaction zone. Hayakawa et al. [42] explored the knowledge of characteristics of ammonia/air flames at the high pressures. Valera-Medina et al.

[43] performed on practical swirl combustors with ammonia fuel mixture to optimise the combustion stability and emission performance.

The major scopes of this paper are not only to choose the best possible configuration with respect to energy efficiency, but also to obtain optimum fuel condition with consideration of lower NOx emissions. It is clear that further efforts are still needed in the NOx concentration reduction in order to avoid an increase in NO. Recently, with the advances in the Additive Manufacturing (3D printing) technologies for micro parts, research efforts are moving toward the optimization of micro combustor by easy and reliable methods. The optimal design is obtained for the first step. In this paper, the micro-combustors with three different wavy profiles are proposed firstly to improve performance. Then the average temperature distribution and uniformity over the outer wall of hydrogen-fuelled micro combustor with different wavy types are compared for various inlet flow velocities. The detailed comparison analysis of the flame structure and temperature distributions in these combustors is carried out to explain the reason of enhancement brought by the improved wavy combustors in comparison with the conventional cylinder combustor (REF). To validate the effect on flame stability of the improved wavy micro-combustor, the blow-out limit is applied to compare and investigate the combustion characteristics of ammonia/hydrogen/air blended between the REF and newly proposed ARC combustors. Finally, the evaluation of reduced NOx emissions efficiency for

wavy micro combustor is performed. The effects of fuel parameters including blended ratio and equivalence ratio on NO_x emissions are also analysed in detail.

2. Methods and Model

2.1 Geometric model

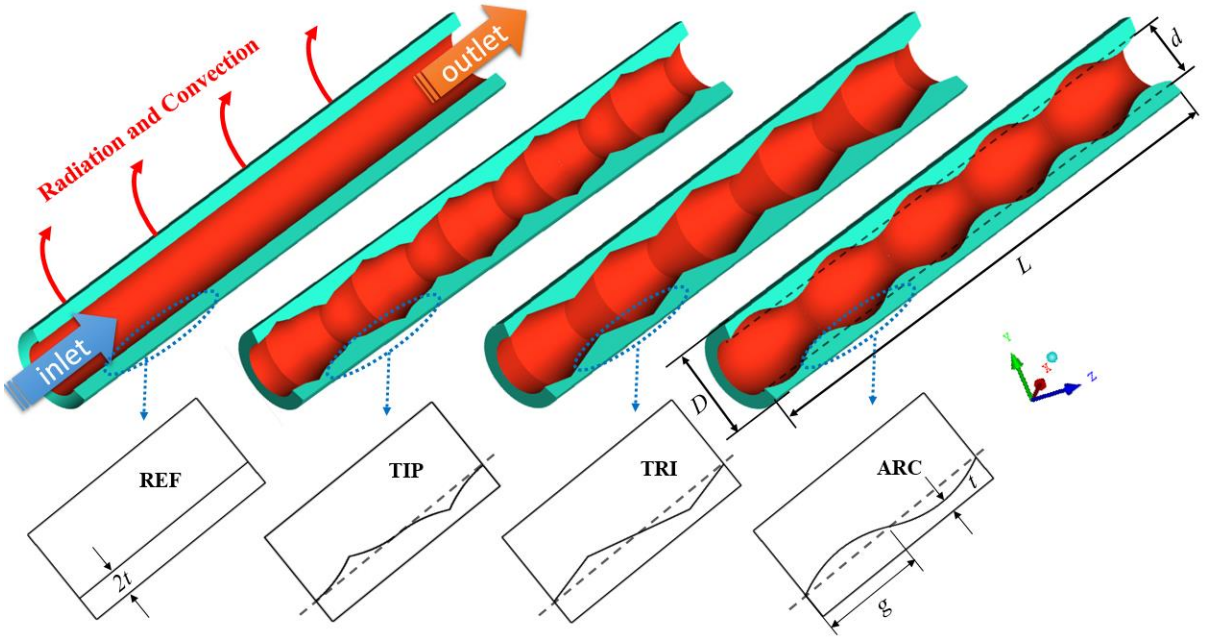

Fig. 1 Schematic diagram of four micro-combustors and partial cross-section view of the four wavy profiles.

The reference micro-combustor is an axisymmetric cylinder for MPG in industrial application. The fuel flows into from the inlet and combustion in the inner circular channel part. Then the energy of radiation and convection is released from the outer wall. The schematic diagram of the micro-combustor without or with the inner wavy profile and their various shapes are presented in Fig. 1. Three improved micro-combustors are designed to keep periodical inner wavy profile. The inner wall of improved combustor has five continuous waves

161 equally spaced in the axial direction. All four combustors with the same fluid
162 region volume are chosen for the present research. The cross-sectional views of
163 all four combustors are shown in Fig. 1. The conversional reference combustor
164 is named REF. The TIP shape is connected by arcs to form a tip, and the TRI
165 shape consists of linear edges of a triangle. The profile of the inner surface of
166 ARC is connected by smooth arcs to facilitate wavy smoothness. During the
167 optimization design of the combustor, the volume of the entire internal channel
168 and wall material are respectively kept constant. The wavy profile is used to
169 change the contact surface between the flame and combustor. The length of the
170 micro-combustor is *L*, the external diameter is *D*, the internal diameter is d, the
171 minimum wall thickness is *t*, and the periodical wavy length is *2g*. The micro-
172 combustors are made of 316 stainless steel whose properties are given in the
173 reference [14]. Table 1 shows detailed dimensions of the combustors.

174 **Table 1. Dimensions of combustor.**

Dimensions	Values (mm)
D	3
d	2
L	20
g	2
t	0.25
wavy periods	5

2.2Mathematical Model

A detailed chemical mechanism and transport based 3D CFD model is adopted in the present numerical investigation. Considerable efforts have been spent to explore thermal performance and reduce NOx emissions of different optimized micro-combustors. All the issues below are mandatory to ensure the accuracy and reliability of the numerical results, e.g. the numerical method, turbulence models, mechanism and boundary conditions, which need to be considered properly. The following issues are considered and assumed before establishing the numerical model [44]: (1) fuel/air mixture steady combustion; (2) considering outer wall radiation and convection; (3) incompressible flows; (4) neglecting surface reaction effect. The fuel inlet Reynolds number can be estimated as Kuo and Ronney [45] modelled for Swiss-roll micro combustors. It is observed that modelling of turbulent flow and transport at Re > 500 is necessary to keep consistency between the experimental and numerical results. Thus the standard k–ε model [31] is used for the turbulent flow and heat transfer in the present study. With the above assumptions, the mathematical model of hydrogen/ammonia/air premixed combustion in micro-combustor is established by using the mass, momentum, energy species and equilibrium law. The related governing equations are written as follows [26].

Mass:

$$\nabla \cdot (\rho \vec{v}) = 0 \tag{1}$$

where ρ is the gas density and $\vec{v}$ is the velocity in the v direction.

Momentum:

$$\rho(\vec{v}\cdot\nabla\vec{v}) = -\nabla p + \nabla\cdot\left(\mu\left[\nabla\vec{v} + (\nabla\vec{v})^T - \frac{2}{3}\nabla\cdot\vec{v}I\right]\right) \quad (2)$$

where p is the gas pressure, μ is the viscosity and I is the unit tensor.

Energy species:

$$\nabla\cdot\vec{v}\left(\rho E_f + p\right) = \nabla\cdot\left[\lambda_{\text{eff}}\nabla T - \left(\sum_j h_j\vec{D}_j\right) + \left(\mu\left[\nabla\vec{v} + (\nabla\vec{v})^T - \frac{2}{3}\nabla\cdot\vec{u}I\right]\right)\cdot\vec{v}\right] + S_f^h \quad (3)$$

where E_f is the total energy, λ_{eff} is the effective thermal conductivity of fluid, ∇T is the temperature difference between fluid and walls. h_j is the enthalpy of species j , $\bar{D}_j$ is the mass diffusion coefficient of species j, $\vec{u}$ is the velocity in the u direction, the and S_f^h is the source term of the fluid enthalpy.

Wall energy equation:

$$\nabla\cdot\left(\lambda_w\cdot\nabla T\right) = 0 \quad (4)$$

where λ_w denotes the conductivity of the combustor surface.

Species equation:

$$\nabla\left(\rho\vec{u}Y_j\right) = -\nabla\vec{D}_j + \omega_j \quad (5)$$

where ω_j and Y_j are the net production rate and the mass fraction of species j.

Ideal gas equation:

$$p = \rho R_g T \tag{6}$$

$$R_g = \frac{R_0}{M} \tag{7}$$

Where R_g denotes the universal gas constant, M is the molecular mass.

The outer wall average temperature:

$$T_{ave} = \frac{\sum A_i T_i}{\sum A_i} \tag{8}$$

The outer wall temperature uniformity is evaluated by the standard deviation parameter of wall temperature σ_T, which can be written as:

$$\sigma_T = \sqrt{\sum_{i=1}^{N} A_i \left(T_i - T_{ave}\right)^2 / \sum_{i=1}^{N} A_i} \tag{9}$$

where A_i and T_i are the area and temperature of outer wall cell i respectively, and T_{ave} is the average temperature of outer wall.

$$Q = h_0 A\left(T_w - T_0\right) + \varepsilon\sigma A\left(T_w^4 - T_0^4\right) \tag{10}$$

Where h_0 is the natural convection coefficient, σ denotes the Stephan-Boltzmann constant which equals to $5.67\times10^{-8}\,\mathrm{W/m^2\cdot K^4}$, ε denotes the emissivity of the combustor wall, T_0 and T_w are the ambient temperature and outer wall temperature respectively.

A specie production expression model for the net rate has to be used to close Eq. (4). The turbulence dissipation e and turbulent kinetic energy k for k-epsilon model are obtained by solving transport equations. The pressure and velocity

coupling are calculated by using SIMPLE algorithm handled by Fluent (Ansys 19.0). These governing equations are solved by the finite volume and the implicit solution method of under-relaxation. A second-order-upwind scheme is used to discretize all governing equations together with the essential relations and proper boundary conditions. Konnov [46] focused on the more detailed mechanism of NH_3 and its product. Kumar and Meyer [47] used the Konnov mechanisms for H_2/NH_3/air mixtures over a wide range equivalence ratios to compare the experimental data and models and evaluate its accuracy. A detailed mechanism model [48] involving 38 species and 232 reactions for hydrogen/ammonia/air gas-phase chemical reaction is verified and achieved by Nakamura and Shindo [49]. It is also the fundamental mechanism model to be applied and verified in the present simulation. The specific heat capacity and mass diffusivity of fuel and air mixture are calculated by the mixing-law and the kinetic-theory respectively. The energy balance between the atmosphere and combustor will be achieved once the flame is stabilized in the micro-combustor. Based on the suggestions from Bongers and De Goey [50] on micro-combustion, Dufour effect is ignored, while Soret effect is considered since it has an impact on NO production rate. The body force and heat transport caused by the concentration gradient are neglected due to their small amount as well as the pressure diffusion[51]. The mass fraction-weighted average of all species is selected for calculations of the mixture gas thermal conductivity and viscosity

242 [52]. The energy equation convergence criterion is set as 10^{-6}, the other
243 continuity, specie and turbulence equations criterion is 10^{-5}.

244 **2.3Computation Domain and Boundary Conditions**

245 The physical computation model contains a fluid domain and a solid domain.
246 For the fluid domain, heat and mass transport of fuel/air mixture along with the
247 chemical reactions are considered. The solid domain takes into account the heat
248 transport encompassing conduction, convection, and radiation. A representative
249 ARC computational domain of the physical system analysed in this study is
250 presented, while other configurations considered in this study such as REF, TIP
251 and TRI are not shown. The mesh schemes of both domains are shown in Fig. 2,
252 in which non-uniform structured mesh is outputted by the pre-processor
253 meshing program ICEM. To obtain a geometric model of the combustor as
254 accurately as possible, various blocks are divided to be close enough to
255 represent the geometric characteristics. These blocks also facilitate the
256 controlling of the number and scale of cells. All correlation vertexes and edges
257 are stitched together into the block of combustor. The cells in all blocks are
258 meshed with high-orthogonality hexahedron, with refinement in the parts of
259 high strains or variations so that the numerical errors can be minimized. Solid
260 domain adopts medium density while fluid domain adopts uses a fine density,
261 because the flame zone within the fluid domain is more complicated than that in
262 the solid domain. In the streamwise direction, a higher mesh distribution is used.

Also, it can be seen that the mesh sizes of the interfaces between the solid domain and fluid domain are nearly the same, which is helpful for the heat transfer couple between the interface of the fluid domain and the solid domain.

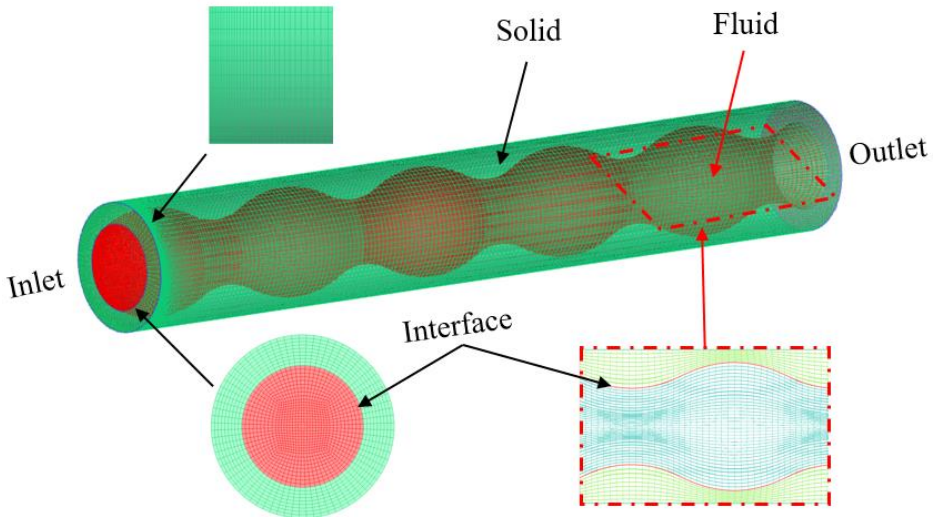

Fig. 2 Geometric domain scheme model and mesh details

From the enlarged region, it is observed that the region near the inlet of both fluid and solid domains has finer mesh than that of other regions. This is because that the gases inject condition from inlet is a significant initial value in the numerical results. The inner surface of solid region and outer fluid domain surfaces are set as interface to interpolate values. The main boundary conditions of all combustor are taken as the velocity-inlet and pressure-outlet respectively. The inlet velocity is variable to evaluate its effect on the combustion performance. The pressure and O_2 mass fraction of outlet are set according to the air condition in atmosphere. All detailed boundary condition settings are generalized in Table 2.

Table 2 Boundary conditions.

Types	Parameters	Values
Inlet	Mass fraction of each species	regard to H_2 or H_2/NH_3 air equivalence ratio(0.6-1.2)
	Velocity (m/s)	regard to cases (8-20)
	Temperature (K)	298
	Turbulent intensity (%)	5
	Hydraulic diameter (mm)	2
Outlet	Gage pressure (Pa)	101325
	Turbulent intensity (%)	5
	Hydraulic diameter (mm)	2
Inner wall	Wall slip	Non-slip
	Thermal condition	Coupled
Outer wall	Material	316 Steel
	Thermal condition	Mixed
	Heat transfer coefficient ($W/(m^2 \cdot K)$)	20

2.4 Model Validation and Mesh Independence Study

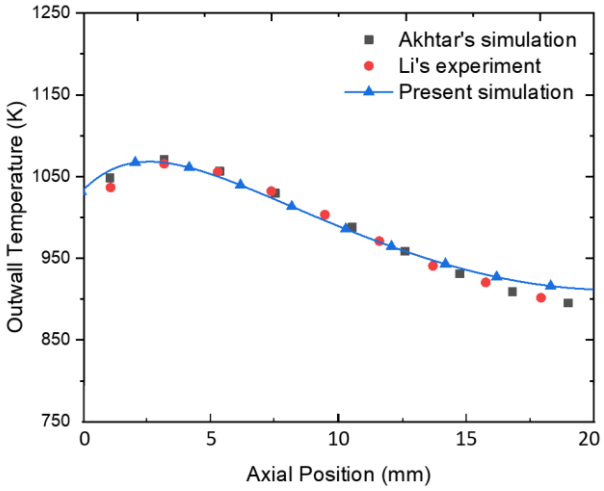

Fig. 3 Comparison of the outer wall temperature between the present simulation and literature data.

The results of the present numerical simulation are compared against the corresponding experimental and numerical data which comes from Li et al. [53] and Akhtar et al. [24] to verify the accuracy of the computational model. The length of the main part combustor from the experimental setup is 20 mm, and a 7 mm inlet is also arranged. The main part combustor size and wall thickness are both the same as the present combustor. In the experimental study of Li et al. [53], temperature distribution of experimental data on outer wall is showed. Akhtar et al. [24] conducted a 2-D axisymmetric numerical simulation on the same micro-combustor too. In this paper, the pure hydrogen case with an inlet velocity of 12m/s and hydrogen/air equivalence ratio of 0.8 is selected. Fig. 3 presents the temperature distribution profiles of the external wall, showing both the experimental and simulation data along the axial direction. It can be seen that the consistence between the present simulation and experimental results

available in the literature is excellent, showing the similar trend of temperature distribution and the position of the temperature peak value. The maximum temperature difference occurs near the combustor outlet, with a value of 19 K, i.e., the maximum relative error between the numerical and experimental results is only 2.1%, which indicates that the computational model established in the present study is reliable.

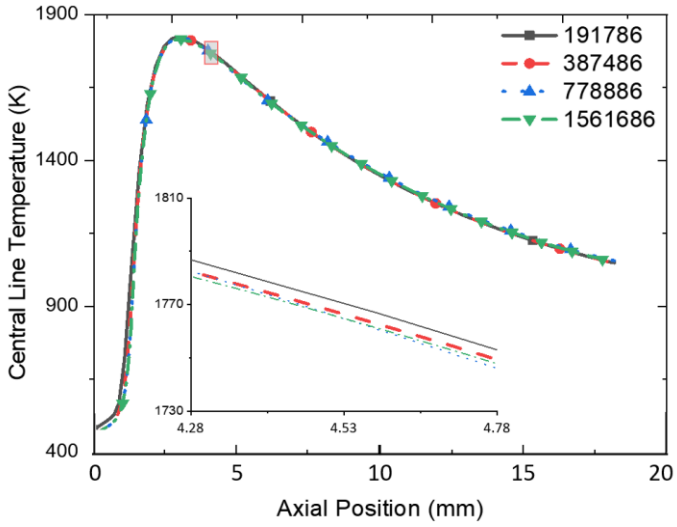

Fig. 4 Distribution of the central line temperature with different grid sizes under the inlet velocity of 12m/s.

To exclude the influence of the grid size on the calculated results, a mesh independence test with 4 different mesh densities ranging from 191,786 to 10,561,686 is conducted. Fig. 4 shows the effect of mesh scale on the central line temperature of the micro combustor where the mixture inlet velocity and the hydrogen/air equivalence ratio are kept at 12m/s and 0.8, respectively. A sizable variation in the central line temperature at streetwise direction for different mesh sizes is observed in the vicinity of the flame, i.e., the flame

distance. The upstream of the flow is also relatively mesh sensitive. By checking the centreline gas temperature profiles of the above meshes (zoomed-in in Fig. 4), it is found that the temperature is a bit decreased with the increase of grid size. It is observed that the mesh with about 387,486 cells is able to well illustrate the gas mixture combustion temperature profiles, and a higher number of cells (778,886) does not yield any significant improvement. It was concluded that the mesh size level of 387,486 cells should be considered suitable for all the following numerical computation sections since it provides a perfect trade-off between the computational accuracy and the time cost. Furthermore, the corresponding mesh size is selected in the present geometrical models with different wavy profiles.

3. Results and Discussion

3.1 Wavy Profile Effect on Thermal Performance

The output of applied energy from micro TPV is proportional to the thermal performance from the outer wall of combustor. The mean wall temperature is a significant symbol of thermal performance, which is defined as the mean value of all cells of the combustor wall. Fig. 5 presents the outer wall mean temperature values of the combustors employing varied wavy profile configurations. In this part, the inlet velocity varies from 8 m/s to 20 m/s, and H_2/air equivalence ratio is set as 0.8. As shown in Fig. 5, with increasing the inlet velocity, the average temperature values increases significantly, whether

the micro-combustor has any wary or not. Under the same equivalence ratio in this section, the increased inlet velocity results in a higher wall temperature. This is because the increasing of the inlet velocity provides a higher energy input, and thus release more heat generation from the combustion. It is clear that the change of wavy type also affects the temperature distribution. It also demonstrates that regardless of the fuel flow velocity, the average temperatures on the wall of TIP, TRI and ARC combustors are higher than that of REF combustor.

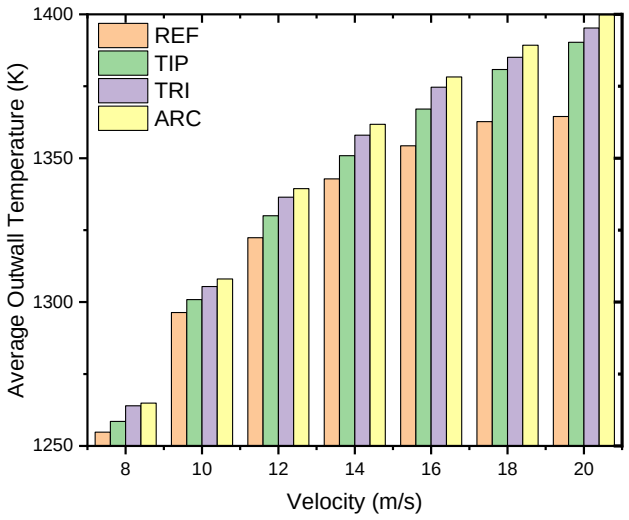

Fig. 5 Average outer wall temperature profiles for different wavy combustors.

The combustor with ARC wavy obtains the highest temperature, while the value of REF combustor is the lowest. The average temperature in REF is increased from 1255K to 1364K as the velocity increases from 8 m/s to 20 m/s. On the contrary, the ARC combustor reaches 1400K at the velocity of 20 m/s. A maximum improvement of 36K can be achieved when comparing the ARC

wavy combustor with the conventional combustor. That is, the improvement of output performance on ARC-TPV is achieved as 10.98%. The improvement of average temperature of wavy is more obvious with the increase of mixture velocity. It should be pointed out that wavy profile enlarges interface between fluid and solid zone for heat transfer. In addition, the average temperature improvement is due to the formation of a recirculation zone on the concave wavy wall which provides more residence time and heating time to stabilize and enhance heat transfer. The viscosity caused turbulence enhances heat transfer between the combustion gas and the solid wall. The thermal performances of the micro-combustors are not only sensitive to the mixture velocity, but also to the change of interior structure area in the combustion chamber.

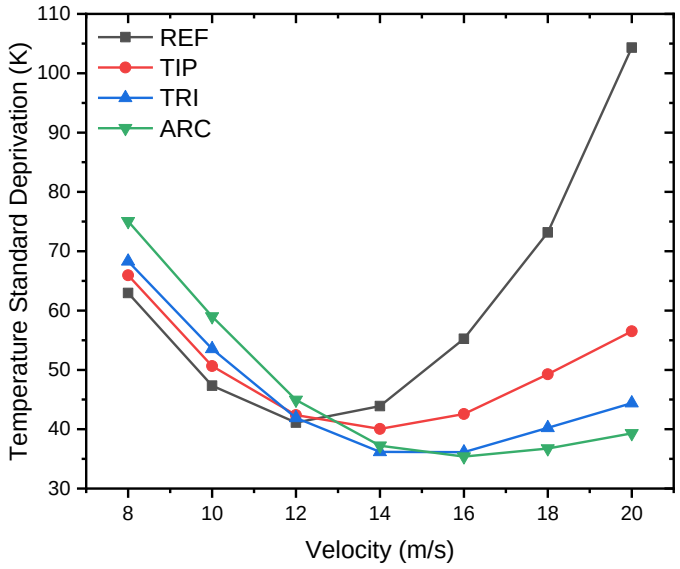

Fig. 6 Non-uniformity of outer wall temperature distribution.

352 The higher and more uniform outer wall temperature has an imperative effect on
353 the radiation efficiency and output power of the micro-TPV system [33]. In
354 order to achieve a high energy conversion efficiency, the wall temperature
355 uniformity must be improved. Furthermore, a uniform temperature distribution
356 reduces outer wall thermal stresses of the micro combustor and prolongs the
357 operation period [54]. In this paper, the temperature standard deviation is
358 measured by calculating uniformity coefficient to quantify the non-uniformity.
359 For this reason, the variation of wall temperature distribution non-uniformity
360 under various inlet velocities is presented in Fig. 6. With an increase of the inlet
361 velocity, the temperature standard deviation (the lower derivation indicates
362 better uniformity) decreases first in the velocity range of 8-12m/s, then
363 increases in the velocity range of 13-20m/s. It can also be observed that
364 temperature standard deviation is very high for REF micro combustor without
365 any wavy. It can be easily observed that the highest standard deviation of about
366 105 K is achieved at the velocity of 20m/s for reference REF combustor. In
367 addition, the non-uniformity coefficient drops down from 42K to 34K due to the
368 implementation of the ARC wavy. Wavy profile is a highly effective measure to
369 improve uniformity when the mixture inlet velocity is higher than 12m/s. The
370 effect of the inner wall on thermal performance is related to the fuel inlet
371 velocity. Although the wavy profile has a negative effect on uniformity at a low
372 speed on, it is obvious that the positive effect is generally much more obvious
373 than the negative effect. This can provide a reference for the further design of

micro-combustor. For temperature uniformity, it is mostly likely due to the increase of local turbulence gradient. The turbulent intensity distribution and for hydrogen-fuelled combustion in REF and ARC combustor are compared. It can be seen that at a lower velocity (8m/s), wavy just causes increasing of turbulence intensity at local bulges. The local turbulence gradient leads to a negative effect on uniformity under lower-inlet-velocity condition. At a higher velocity (20m/s), the turbulence intensity is enforced over a wide area rather limited in local area. It is attributed to the fact that the positive effect of wavy profile is sizable enough to change the fluid movement towards the outlet and enhance the heat transfer between the combustion chamber wall and the combustion gas.

Fig. 7 shows the outer wall temperature distribution and non-uniformity for 20%NH3+80%H2 blended fuelled combustion. These trends are similar to the above-mentioned pure hydrogen combustion. According to the foregoing analysis, ARC is a better configuration for either hydrogen/air or ammonia/hydrogen/air fuelled combustion considering temperature uniformity and average temperature.

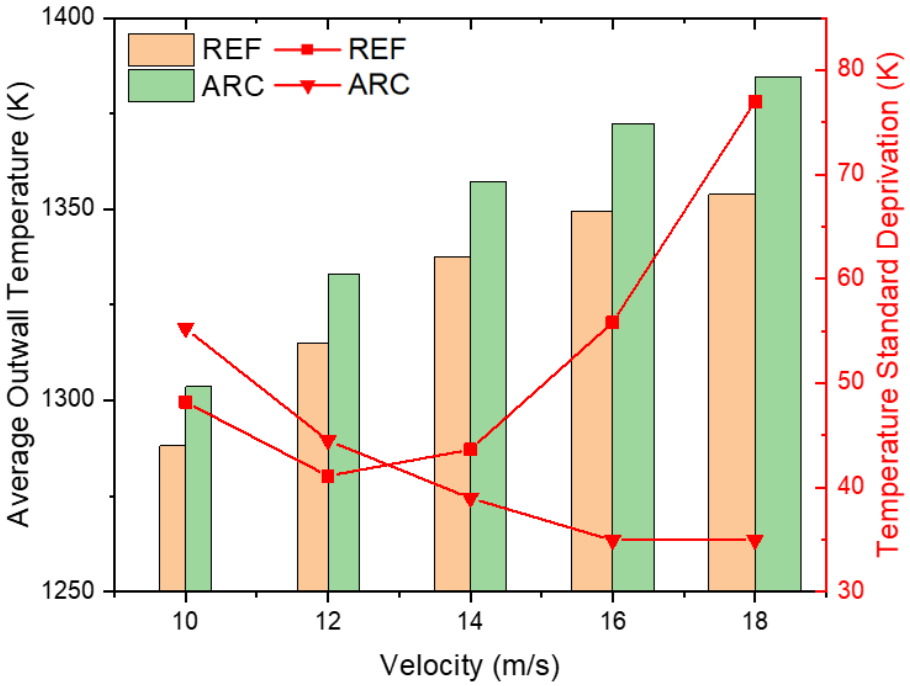

Fig. 7 Outer wall temperature distribution and non-uniformity for 20%NH_3+80%H_2 fuelled.

3.2 Thermodynamics characteristics

To explore the detailed effects of wavy profile on both wall temperature distribution and flame temperature, contours of flame temperature field variation of middle cross section on four combustors are shown in Fig.8, where fuel flow velocity and equivalence ratio are set as 20m/s and 0.8, respectively. High temperature values associated with wavy wall are mainly rooted in the above mentioned thermal performance. Convergent-divergent flow channel with wavy profile affects inner reactants velocity, provides more residence time and heating time, and makes a fundamental change in the interaction amplitude between the wall and the shape of the flame evolution. To further analyze the basic mechanism that leads to the difference in temperature distribution of the four kinds of micro-combustors, several radial cross-section temperature

distributions under different combustor structures are revealed. The wall temperature at X=2 cross section of the REF micro–combustor is lower than that of the other three combustors. The wall temperature distribution at X=8 and 10 of the TRI and ARC micro-combustor is more homogeneous. The reason for these abovementioned phenomena is that the flame radial is narrowed by the internal wavy profile. The flame front is compressed shorter and the ignition zone (green zone in the contour) is broadened.

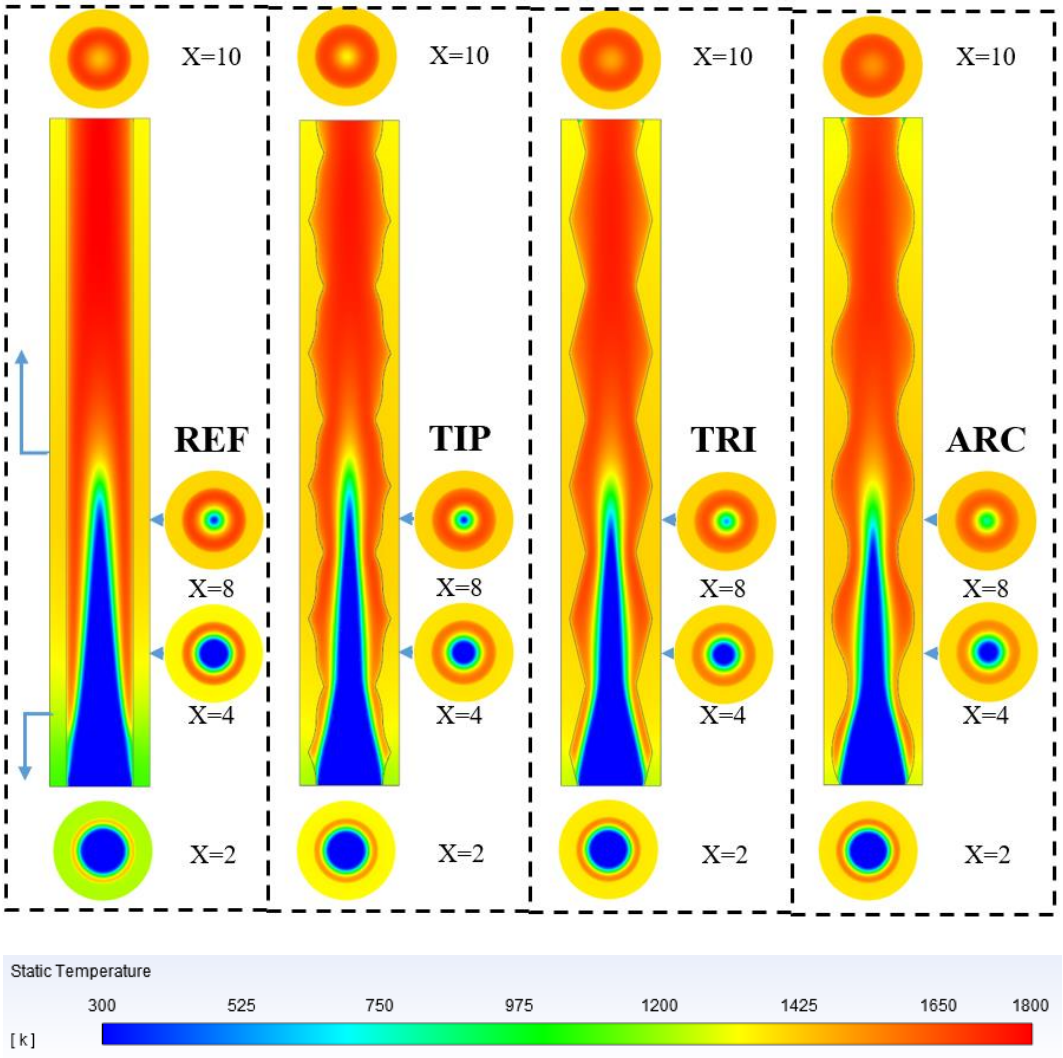

Fig. 8 Variation of the temperature field.

412 It is worthwhile to mention that under the same fuel flow rate, the increase in
413 combustion gas velocity due to the periodical change of inlet area does result in
414 a higher temperature of outer wall near the inlet compared to REF combustor.
415 This phenomenon shows that the wavy arrangement is beneficial to the
416 preheating of the mixture by the higher temperature inlet wall. In general, the
417 variation resulted in a more intensive heat transfer between the solid wall and
418 combustion gas.

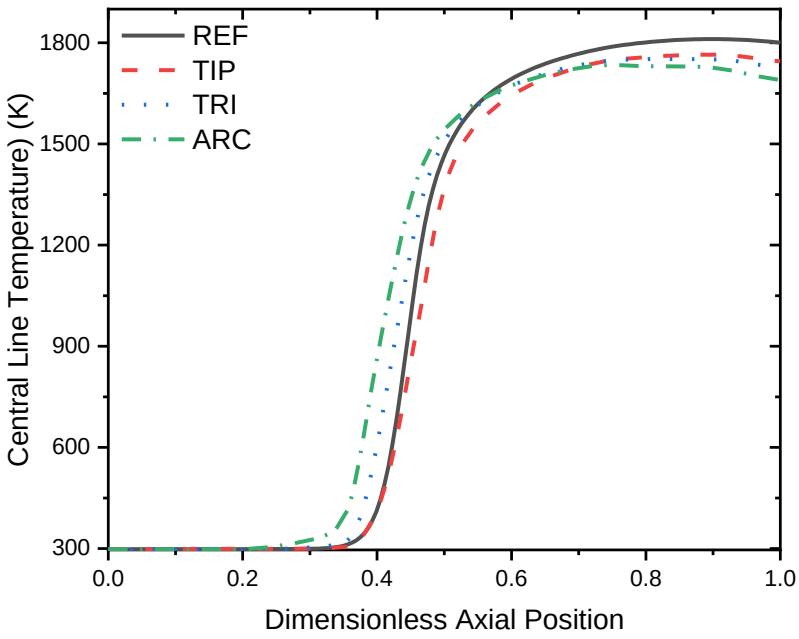

Fig. 9 Temperature profiles along the central line of different wavy profile shapes.

419 Fig. 9 compares the temperature profiles along the central line in the four above
420 mentioned combustors. The flame reaction zones in TRI and ARC are almost
421 located in the upstream region along the central line due to the function of two
422 wavy profiles. However, the flame front edge moves downstream with the

implementation of TIP wavy profile. The flame location is sensitive to gas velocity. After checking the velocity distribution of the combustor cross section, it can be seen that the wavy wall has an obvious influence on the flow velocity. The front edge of the flame is located in the middle of the combustor, which is exactly in the accelerating area of the gas from the contraction passage. It can be concluded that the acceleration area at the TIP's central passage is closer to the downstream. Thus the flame front edge region moves downstream with the implementation of the TIP wavy profile comparing with TRI and ARC. Meanwhile, it can be observed that the highest flame temperature decreases with the function of wavy profile because more area is used to transfer heat to the outer solid walls. It can also be seen that the change of the inner temperature is consistent with the variation of the temperature field in Fig. 8.

3.3 Flammability Behaviour

Fig. 10 presents the combustion states of REF and ARC micro-combustors with different hydrogen/ammonia mass blend ratios and velocities. Combustion states are similar in cases of 100% hydrogen and 80%H_2+20%NH_3. REF and ARC have the same flammability. As the blend proportion of H_2 decreases to lower than 80%, the combustion states in REF begin to blow out. Moreover, the value of blow out limit becomes smaller with the decrease of H_2. The blow out limits of REF micro-combustor operation on 60%H_2+40%NH_3 and 40%H_2+60%NH_3 are 10 m/s and 16m/s, respectively. This indicates that

ammonia has a lower flame velocity than hydrogen. Beyond the blow out limit, the flames attached to the inner combustor fail to keep stable and contracts down toward complete extinction. Additionally, by comparing the combustion states of ARC combustor, the most obvious difference is revealed: ARC can combust stably in any fuel mixture ratio or velocity due to the varied velocities and longer residence time in channel. This is attributed to the preheat-process of wall on the hydrogen-fuel, and turbulence enhances the flame stability. The present simulation results shows that the hydrogen can combust with inlet velocity of 20m/s. If the ammonia ratio in the mixture-fuel rises to a certain level, the flame even will be blown out at 12m/s. Therefore, a micro-combustor with ARC is more favourable to expand the blow out limit and anchor flame than the conventional REF combustor.

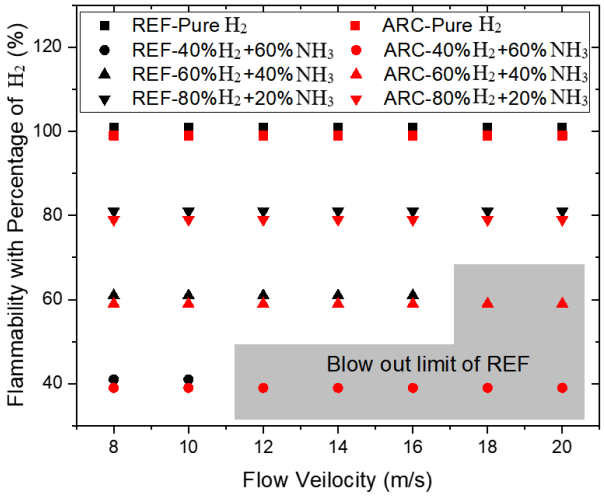

Fig. 10 Blowout limit of REF and ARC with different hydrogen/ammonia mixture and velocities.

3.4 NOx Emissions Reduction

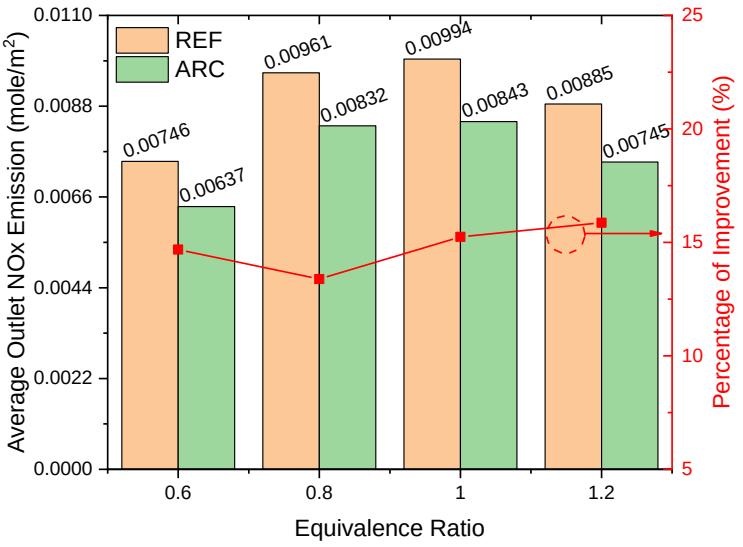

Fig. 11 Variation of NOx emissions under different equivalence ratios of H_2/NH_3.

For combustion with enhanced performance, NOx control and emission reduction technology is also a relatively complex issue. Fig. 11 attempts to verify the role of wavy structure on NOx pollution prevention of the exhaust gas by using 60%H_2+40%NH_3 mixture fuel in REF and ARC combustors. Both REF and ARC combustors have the same area of outlet. Effects of combustor with wavy or without, and equivalence ratio are examined in this section. The nitrogen oxide analysis of the outlet exhaust gas shows that the content of NO_2 is almost zero emission, but there is more NO. The NO is represented as the NOx emission for following analysis. In the field of micro combustor, the off-stoichiometric condition is intentionally used to protect the combustor wall from hot combustion gases. Equivalence ratio of fuel flow for combustion has been correlated to the amount of NOx generated. To understand the NOx emission

characteristics for various conditions, the global equivalence ratio is varied in the range of 0.6~1.2 together with the change of combustor configuration. With equivalence ratio increasing from 0.6 to 1.2, the REF combustor outlet NOx emission increases from 0.00746 mol/m^2 to 0.00994mol/m^2, then decreases to 0.00885 mol/m^2, the peak emission value is at stoichiometric equivalence ratio of 1.0. Regardless of the fuel equivalence ratio, applying the ARC wavy to fuel-lean and fuel-rich stoichiometric zone can strongly reduce NOx content of exhaust gas. The relative improvement in NOx emissions with ARC wavy profile is kept utmost at 13.4-15.9% compared to REF combustor. Thus, micro combustor design with ARC wavy that provides highly reduced NOx emission is determined.

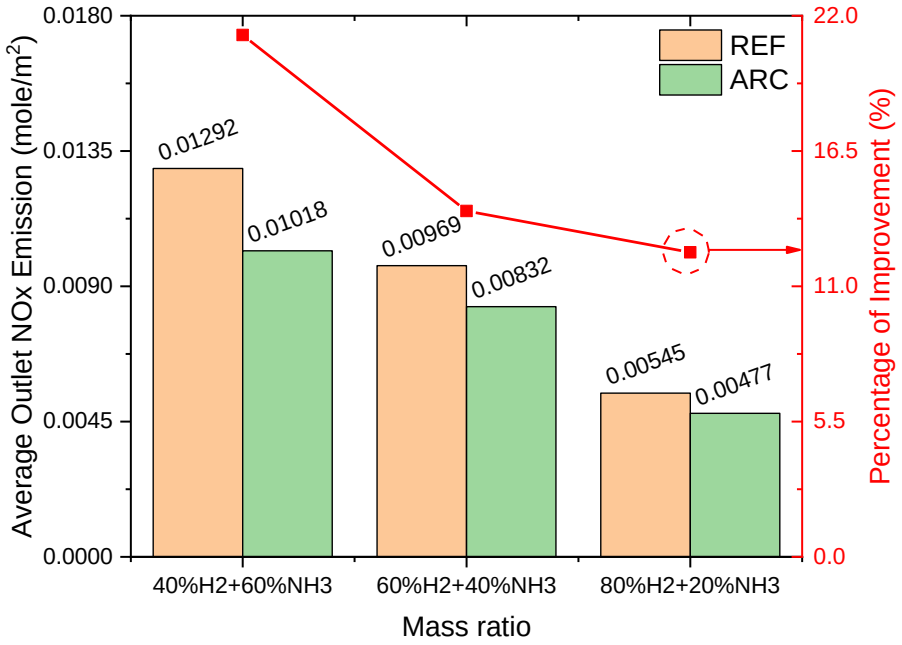

Fig. 12 Variation of NOx emissions under different mixture ratios of H_2/NH_3.

To explore the effect of fuel mixture ratio on NOx reduction efficiencies, NOx emission level in different mixture ratios is investigated. Fig. 12 shows the variation of the generated NOx under different mixture ratios of H_2 and NH_3. All NOx emission from the outlet of ARC combustor is much lower than that of the REF combustor under the same operating conditions. Average outlet NOx emission is yielded with an inlet velocity of 12m/s and equivalence ratio of 0.8 for mixture fuel ratio $40\%H_2+60\%NH_3$, $60\%H_2+40\%NH_3$ and $40\%H_2+60\%NH_3$ with relative conversion of fuel ammonia to NOx at 21.2%, 14.1% and 12.3% respectively. The relative improvement percentage gradually increases with the increase of the nitrogen fuel mass ratio. The combustor with wavy radiates more heat for energy conversion, so the gas inside is at a lower temperature. This main pathway of NO_X formation mechanism is as following reaction: $N2 + O \rightleftharpoons NO + N$. Lower temperatures lead to lower O and NO production. It can also be seen from Section 3.4 that the decrease in the proportion of hydrogen will lead to more reduction of NO emission. This is due to the obviously decrease of gas temperature. This also demonstrates that lower gas temperatures are conducive to emissions improvement. From the present simulation data, it is evident that when the combustor improving techniques are advanced such as normal internal wall of REF is substituted with ARC wavy, a subsequent difference in NOx formation is seen resulting in higher NOx reduction efficiencies.

4. Conclusions

In this work, in order to enhance the thermal performance and reduce the NOx emission of the micro-combustor for thermophotovoltaic application, 3D numerical investigations are conducted to evaluate the thermal and NOx emission performances of the modified micro-combustors with a wavy profile. The model with detailed ammonia/hydrogen/air reaction mechanisms is validated first with experimental data available in the literature. Three different wavy profiles, i.e. TIP, TRI and ARC, are considered, as the NH_3-H_2 mixture flow velocity and equivalence ratio is varied. The impact of such wavy configurations on enhancing the thermal performance, improving flame stabilization and reducing the NOx emissions is evaluated to obtain an optimum design of a micro-combustor. Key findings are summarized as:

1. The average temperature of the outer wall of the proposed wavy micro combustors (no matter whether the shape is TIP, TRI or ARC) is higher than that of the conventional micro-combustor, regardless of the hydrogen flow velocity. Furthermore, maximum wall temperature is found to be associated with ARC wavy micro combustor. The temperature difference between ARC and the conventional combustor is approximately 36K.
2. The maximum standard deviation of the average temperatures is about 105 K, when the inlet flow velocity is set to 20m/s in reference to the

conventional combustor. The minimum non-uniformity coefficient is found to be decreased from 42K to 34K, when considering the ARC wavy configuration. The wavy profile is shown to be more effective on improving temperature uniformity, when the mixture velocity is higher than 12m/s.

3. The blowout limits of the conventional micro-combustors operating on the conditions of 60%H_2+40%NH_3 and 40%H_2+60%NH_3 are 10 m/s and 16m/s, respectively. ARC micro-combustor is found to be more efficient in anchoring flame and expanding the blowout limit to more than 20m/s than the conventional design.
4. Regardless of the equivalence ratio, applying the ARC wavy to fuel-lean and fuel-rich stoichiometric zone can strongly reduce NOx emission found in the exhaust combustion gas. The relative reduction in NOx emissions with ARC wavy profile is found to be in the range of 13.4-15.9% in comparison with the conventional micro-combustor.
5. NO_x emission efficiencies at the combustor outlet under the tested conditions of 40%H_2+60%NH_3, 60%H_2+40%NH_3 and 40%H_2+60%NH_3 are shown to be 21.2%, 14.1% and 12.3% respectively. Further NOx emission reduction is found to gradually increase with the increase of the NH_3 mass ratio.

In general, the present work sheds lights on the design of a wavy-shaped micro-combustor with enhanced thermal performance and reduced NO_x emission.

Conflict of interest statement

The authors declared that they have no conflicts of interest to this work.

Acknowledgments

This work was funded by International Graduate Exchange Program of Beijing Institute of Technology and supported by University of Canterbury under grant number 452STUPDZ. Lei Han would like to thank the University of Canterbury for hosting his PhD exchange studentship in the group of Dr. Dan Zhao.

References

[1] Valera-Medina A, Xiao H, Owen-Jones M, David WIF, Bowen PJ. Ammonia for power. PrECS 2018;69:63-102.

[2] Lee SI, Um DH, Kwon OC. Performance of a micro-thermophotovoltaic power system using an ammonia-hydrogen blend-fueled micro-emitter. International Journal of Hydrogen Energy 2013;38(22):9330-42.

[3] Chou SK, Yang WM, Chua KJ, Li J, Zhang KL. Development of micro power generators – A review. Applied Energy 2011;88(1):1-16.

[4] Kang X, Veeraragavan A. Experimental demonstration of a novel approach to increase power conversion potential of a hydrocarbon fuelled, portable, thermophotovoltaic system. Energy Conversion and Management 2017;133:127-37.

[5] Su Y, Song J, Chai J, Cheng Q, Luo Z, Lou C, et al. Numerical investigation of a novel micro combustor with double-cavity for micro-thermophotovoltaic system. Energy Conversion and Management 2015;106:173-80.

[6] Ju Y, Maruta K. Microscale combustion: Technology development and fundamental research. PrECS 2011;37(6):669-715.

[7] Kobayashi H, Hayakawa A, Somarathne KDKunkuma A, Okafor Ekenechukwu C. Science and technology of ammonia combustion. Proceedings of the Combustion Institute 2019;37(1):109-33.

[8] Ma L, Xu H, Wang X, Fang Q, Zhang C, Chen G. A novel flame-anchorage micro-combustor: Effects of flame holder shape and height on premixed CH4/air flame blow-off limit. Applied Thermal Engineering 2019;158.

[9] Wan J, Fan A, Yao H, Liu W. Effect of thermal conductivity of solid wall on combustion efficiency of a micro-combustor with cavities. Energy Conversion and Management 2015;96:605-12.

[10] Pan JF, Wu D, Liu YX, Zhang HF, Tang AK, Xue H. Hydrogen/oxygen premixed combustion characteristics in micro porous media combustor. Applied Energy 2015;160:802-7.
[11] Bani S, Pan J, Tang A, Lu Q, Zhang Y. Numerical investigation of key parameters of the porous media combustion based Micro-Thermophotovoltaic system. Energy 2018;157:969-78.
[12] Yilmaz H. Investigation of combustion and emission performance of a micro combustor: Effects of bluff body insertion and oxygen enriched combustion conditions. International Journal of Hydrogen Energy 2019;44(47):25985-99.
[13] Nadimi E, Jafarmadar S. The numerical study of the energy and exergy efficiencies of the micro-combustor by the internal micro-fin for thermophotovoltaic systems. Journal of Cleaner Production 2019;235:394-403.
[14] Pan J, Zhang C, Pan Z, Wu D, Zhu Y, Lu Q, et al. Investigation on the effect of bluff body ball on the combustion characteristics for methane/oxygen in micro combustor. Energy 2020;190.
[15] Yan Y, Wu G, Huang W, Zhang L, Li L, Yang Z. Numerical comparison study of methane catalytic combustion characteristic between newly proposed opposed counter-flow micro-combustor and the conventional ones. Energy 2019;170:403-10.
[16] Peng Q, Yang W, E J, Xu H, Li Z, Tay K, et al. Investigation on premixed H2/C3H8/air combustion in porous medium combustor for the micro thermophotovoltaic application. Applied Energy 2020;260.
[17] Peng Q, Yang W, E J, Xu H, Li Z, Yu W, et al. Experimental investigation on premixed hydrogen/air combustion in varied size combustors inserted with porous medium for thermophotovoltaic system applications. Energy Conversion and Management 2019;200.
[18] Peng Q, E J, Chen J, Zuo W, Zhao X, Zhang Z. Investigation on the effects of wall thickness and porous media on the thermal performance of a non-premixed hydrogen fueled cylindrical micro combustor. Energy Conversion and Management 2018;155:276-86.
[19] Zuo W, E J, Lin R. Numerical investigations on an improved counterflow double-channel micro combustor fueled with hydrogen for enhancing thermal performance. Energy Conversion and Management 2018;159:163-74.
[20] Tang A, Cai T, Huang Q, Deng J, Pan J. Numerical study on energy conversion performance of micro-thermophotovoltaic system adopting a heat recirculation micro-combustor. Fuel Process Technol 2018;180:23-31.
[21] E J, Han D, Deng Y, Zuo W, Qian C, Wu G, et al. Performance enhancement of a baffle-cut heat exchanger of exhaust gas recirculation. Applied Thermal Engineering 2018;134:86-94.
[22] Yan Y, Xu F, Xu Q, Zhang L, Yang Z, Ran J. Influence of controllable slit width and angle of controllable flow on hydrogen/air premixed combustion characteristics in micro combustor with both sides–slitted bluff body. International Journal of Hydrogen Energy 2019;44(36):20482-92.
[23] Li Y-H, Hong J-R. Performance assessment of catalytic combustion-driven thermophotovoltaic platinum tubular reactor. Applied Energy 2018;211:843-53.
[24] Akhtar S, Kurnia JC, Shamim T. A three-dimensional computational model of H2–air premixed combustion in non-circular micro-channels for a thermo-photovoltaic (TPV) application. Applied Energy 2015;152:47-57.
[25] Zuo W, Zhang Y, Li J, Li Q, He Z. A modified micro reactor fueled with hydrogen for reducing entropy generation. International Journal of Hydrogen Energy 2019;44(51):27984-94.
[26] Mansouri Z. Combustion in wavy micro-channels for thermo-photovoltaic applications – Part I: Effects of wavy wall geometry, wall temperature profile and reaction mechanism. Energy Conversion and Management 2019;198.
[27] Cai T, Tang A, Zhao D, Zhou C, Huang Q. Experimental observation and numerical study on flame structures, blowout limit and radiant efficiency of premixed methane/air in micro-scale planar combustors. Applied Thermal Engineering 2019;158.

[28] Wang Y, Zhou Z, Yang W, Zhou J, Liu J, Wang Z, et al. Instability of flame in micro-combustor under different external thermal environment. Exp Therm Fluid Sci 2011;35(7):1451-7.
[29] Jiang D, Yang W, Chua KJ, Ouyang J. Thermal performance of micro-combustors with baffles for thermophotovoltaic system. Applied Thermal Engineering 2013;61(2):670-7.
[30] Emadi A, Emami MD. Analysis of entropy generation in a hydrogen-enriched turbulent non-premixed flame. International Journal of Hydrogen Energy 2013;38(14):5961-73.
[31] Zhao D, Guan Y, Reinecke A. Characterizing hydrogen-fuelled pulsating combustion on thermodynamic properties of a combustor. Communications Physics 2019;2(1).
[32] He Z, Yan Y, Xu F, Yang Z, Cui H, Wu Z, et al. Combustion characteristics and thermal enhancement of premixed hydrogen/air in micro combustor with pin fin arrays. International Journal of Hydrogen Energy 2020.
[33] Peng Q, Wu Y, E J, Yang W, Xu H, Li Z. Combustion characteristics and thermal performance of premixed hydrogen-air in a two-rearward-step micro tube. Applied Energy 2019;242:424-38.
[34] Zuo W, Li J, Zhang Y, Li Q, Jia S, He Z. Multi-factor impact mechanism on combustion efficiency of a hydrogen-fueled micro-cylindrical combustor. International Journal of Hydrogen Energy 2020;45(3):2319-30.
[35] Alipoor A, Saidi MH. Numerical study of hydrogen-air combustion characteristics in a novel micro-thermophotovoltaic power generator. Applied Energy 2017;199:382-99.
[36] Fajri HR, Jafari MJ, Shamekhi AH, Jazayeri SA. A numerical investigation of the effects of combustion parameters on the performance of a compression ignition engine toward NOx emission reduction. Journal of Cleaner Production 2017;167:140-53.
[37] Cai T, Zhao D, Wang B, Li J, Guan Y. NO emission and thermal performances studies on premixed ammonia-oxygen combustion in a CO2-free micro-planar combustor. Fuel 2020;280.
[38] Xiao H, Valera-Medina A, Marsh R, Bowen PJ. Numerical study assessing various ammonia/methane reaction models for use under gas turbine conditions. Fuel 2017;196:344-51.
[39] da Rocha RC, Costa M, Bai X-S. Chemical kinetic modelling of ammonia/hydrogen/air ignition, premixed flame propagation and NO emission. Fuel 2019;246:24-33.
[40] Filipe Ramos C, Rocha RC, Oliveira PMR, Costa M, Bai X-S. Experimental and kinetic modelling investigation on NO, CO and NH3 emissions from NH3/CH4/air premixed flames. Fuel 2019;254.
[41] Li S, Zhang S, Zhou H, Ren Z. Analysis of air-staged combustion of NH3/CH4 mixture with low NOx emission at gas turbine conditions in model combustors. Fuel 2019;237:50-9.
[42] Hayakawa A, Goto T, Mimoto R, Arakawa Y, Kudo T, Kobayashi H. Laminar burning velocity and Markstein length of ammonia/air premixed flames at various pressures. Fuel 2015;159:98-106.
[43] Valera-Medina A, Marsh R, Runyon J, Pugh D, Beasley P, Hughes T, et al. Ammonia–methane combustion in tangential swirl burners for gas turbine power generation. Applied Energy 2017;185:1362-71.
[44] Jiaqiang E, Zuo W, Liu X, Peng Q, Deng Y, Zhu H. Effects of inlet pressure on wall temperature and exergy efficiency of the micro-cylindrical combustor with a step. Applied Energy 2016;175:337-45.
[45] Kuo C, Ronney P. Numerical modeling of non-adiabatic heat-recirculating combustors. Proceedings of the Combustion Institute 2007;31(2):3277-84.
[46] Konnov AA. Implementation of the NCN pathway of prompt-NO formation in the detailed reaction mechanism. Combustion and Flame 2009;156(11):2093-105.
[47] Kumar P, Meyer TR. Experimental and modeling study of chemical-kinetics mechanisms for H2–NH3–air mixtures in laminar premixed jet flames. Fuel 2013;108:166-76.

[48] Nakamura H, Hasegawa S, Tezuka T. Kinetic modeling of ammonia/air weak flames in a micro flow reactor with a controlled temperature profile. Combustion and Flame 2017;185:16-27.
[49] Nakamura H, Shindo M. Effects of radiation heat loss on laminar premixed ammonia/air flames. Proceedings of the Combustion Institute 2019;37(2):1741-8.
[50] Cai T, Tang A, Zhao D, Zhou C, Huang Q. Flame dynamics and stability of premixed methane/air in micro-planar quartz combustors. Energy 2020;193.
[51] Cai T, Zhao D, Li X, Shi B, Li J. Mitigating NO emissions from an ammonia-fueled micro-power system with a perforated plate implemented. J Hazard Mater 2021;401.
[52] Zuo W, E J, Peng Q, Zhao X, Zhang Z. Numerical investigations on thermal performance of a micro-cylindrical combustor with gradually reduced wall thickness. Applied Thermal Engineering 2017;113:1011-20.
[53] Li J, Chou SK, Yang WM, Li ZW. Experimental and numerical study of the wall temperature of cylindrical micro combustors. JMiMi 2009;19(1).
[54] Zhao X, E J, Zhang Z, Chen J, Liao G, Zhang F, et al. A review on heat enhancement in thermal energy conversion and management using Field Synergy Principle. Applied Energy 2020;257.